

REPRESENTATION OF STRUCTURAL SOLUTIONS IN BLENDED WING BODY PRELIMINARY DESIGN

L. U. Hansen, W. Heinze, P. Horst
 IFL - Institut für Flugzeugbau und Leichtbau
 (Institute of Aircraft Design and Lightweight Structures)
 TU Braunschweig, Germany

Keywords: *Blended Wing Body (BWB), flying wing, structural design, preliminary design*

Abstract

The structural analysis of Blended Wing Body (BWB) aircraft configurations is presented in the context of a preliminary aircraft design process with the aircraft design and optimization program PrADO of the IFL.

A process is described that enables parametric creation of detailed Finite Element models, its load cases and loads: Iteratively different flight conditions are trimmed and corresponding pressure distributions calculated by the higher-order sub- and supersonic panel code HISSS (EADS-M). Each defined loading condition is used for the iterative structural sizing of the primary structure. Based on Finite Element idealization a mass estimation of all structural masses is performed. The primary and secondary masses are fed back into the closed overall aircraft optimization loop of PrADO until this iterative procedure shows convergence on calculated aircraft variables (e.g. aircraft masses and static engine thrust).

Examples of different structural solutions and their integration in the global model are presented for passenger versions of a 700PAX BWB with a special consideration of a pressurized cabin. Structural masses and parametric studies on the influence of the centre body rib spacing are presented and compared by their weight breakdowns.

1 Introduction

Fuel prices and their increasing share in operational costs enforce developments of

efficient alternatives to today's transport aircraft configurations. Although aircraft designs have been greatly improved with each generation, the major design characteristics remained unchanged.

Fuel efficiency and environmental friendliness are likely to be of high importance for future aircraft designs. Preliminary studies have shown a potential for certain unconventional aircraft configurations with a reduction in fuel consumption and thus an increase in economic efficiency. One of the promising designs is based on the idea of a flying wing (FW) with a centre wing replacing the conventional fuselage. The expectations of the FW designs are based on the favorable effect of the lifting central body and a supposedly lower wetted surface [6]. The aerodynamic loads are created partly at the location of the payload weight. This reduces bending moments and might lower the structural mass of the final configuration. On the other hand the pressurization loads of the passenger cabin are creating an unfavorable loading condition of the fuselage with its non-circular cross-section. This might have a contrary, negative effect on the achievable primary mass of the structure. One type of FW configurations are the BWB aircraft that are a blended arrangement of fuselage body, wing and in some cases vertical and horizontal tail planes or canards.

The high level of functional integration requires a multidisciplinary design approach, for an objective assessment of the advantages, that is based on analytical theories and methods instead of empirical relations. Wakayama and

Kroo [13] describe that the challenges to the multidisciplinary design optimization (MDO), “...have been identified in the breadth and depth of the analysis desired to capture aerodynamic, stability, and control issues for this configuration.”. Liebeck presents in [6], [7] and [8] extracts of multidisciplinary design tasks that contain advanced methods for all disciplines including structure. The results presented therein include predictions for the reduction in fuel consumption and operational empty weight. In [6] and [8] two BWB designs are compared to the conventional aircraft with the result of -32% fuel burn and -19% operating empty weight (OEW) (480 passenger (PAX), range 8700 nm) and -27% fuel burn and -12% OEW (800 PAX, range 7000 nm).

The strong relation between aircraft weight and fuel consumption shows the sensitivity of such predictions, especially, if a strong interaction between the disciplines exists.

2 Weight Prediction Methodology

Due to the great influence of the structural weight on the overall performance of such aircraft, the mass prediction of the in-house design tool PrADO (Preliminary Aircraft Design and Optimization Program, W. Heinze [5]) has been significantly enhanced to calculate the structural mass of BWB primary structure. Fig. 1 shows areas of a BWB configuration where changes to the prediction methods were required.

MDO weight prediction methods often rely on statistical data that cover existing aircraft. Different relations can be determined for each component of the aircraft and the accuracy is obtained by calibration to detailed weight breakdowns of existing aircraft. A disadvantage of such weight prediction is the lack of a physics-based aircraft, geometry and loading conditions’ representation. The statistical basis of such methods limits applicability, if fundamental changes to the configuration have taken place (e.g. BWB aircraft).

Another common practice is the combination of statistical and analytical methods. For example, system and furnishing masses are predicted by statistical means, while the mass of the primary structure is described by simple mechanical models. The structure is often simplified by beam models representing the wing, tail planes and fuselage. Loads are calculated and distributed by general assumptions (rigid body elements, interpolation elements, etc.) and the fuselage pressurization is often neglected.

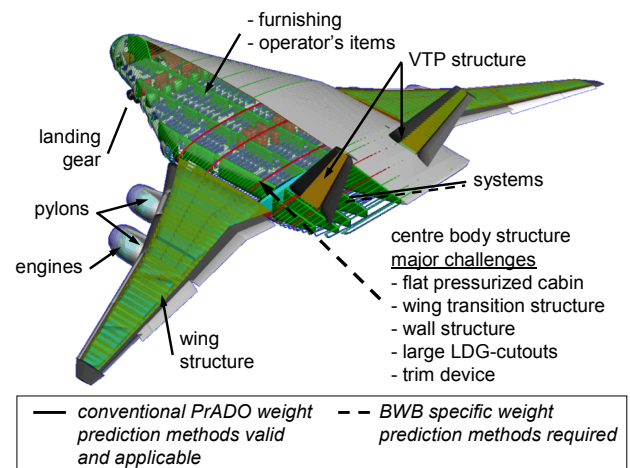


Fig. 1. Major challenges in weight prediction of BWB configurations

In comparison with conventional aircraft configurations, the BWB concepts show a different fuselage loading condition. Large pressurization loads act on the flat cabin and hence on the fuselage structure. The wing bending is not carried by a centre-box, but rather by large wing attachment frames and a wing-transition structure. The integral design and the differences in loading compared to conventional aircraft require physics-based prediction methods that include a high level of design integration through a consideration of all involved disciplines.

In order to cope with these requirements, a method for conventional airplane configurations described in [11] and [12] has been modified to represent BWB structures. This method is based on a complete parametric aircraft description and implemented as a module in the multidisciplinary design program PrADO.

3 Preliminary Multidisciplinary Aircraft Design with the Tool PrADO

3.1 Introduction

The in-house preliminary aircraft design and optimization program PrADO [5] of the *Institut für Flugzeugbau und Leichtbau (IFL), TU Braunschweig* is an arrangement of modules that cover all aspects of the preliminary aircraft design process. A common description of the aircraft and an exchange of information between design modules is performed via a database management system (DMS) which includes all independent (e.g. design requirements defined by the user) and dependent design variables (e.g. results of all previously performed design modules).

Starting with an initial parametric definition of the aircraft the sequential design process covers all major aspects that are relevant to simulate a complete design process of an aircraft and to calculate its properties and performance. The major design modules, as shown in Fig. 2, comprise of aircraft and component geometry, aerodynamics, flight mission simulations, structural analysis, weight prediction, performance and trim calculations. The design process iterates until convergence of dependent variables is achieved. Result of the process is an aircraft description which gives information about the aircraft performance and properties.

Three analysis modes are available in PrADO to perform either a single converged design, a multiparametric study or an optimization of multiple parameters.

In detail, the following steps are performed sequentially:

1. Design requirements of the configuration are summarized and completed.
2. Aircraft geometry is calculated based on the parametric aircraft description.
3. An aerodynamic panel model of the airplane is created and maps of aerodynamic coefficients are generated for the whole flight regime. The results are calculated with the higher order sub

and supersonic panel code HISSS ([3], EADS-M) with additional drag corrections to account for the zero lift drag of the aircraft. The aerodynamic properties are needed for flight simulations to predict performance, control and stability properties.

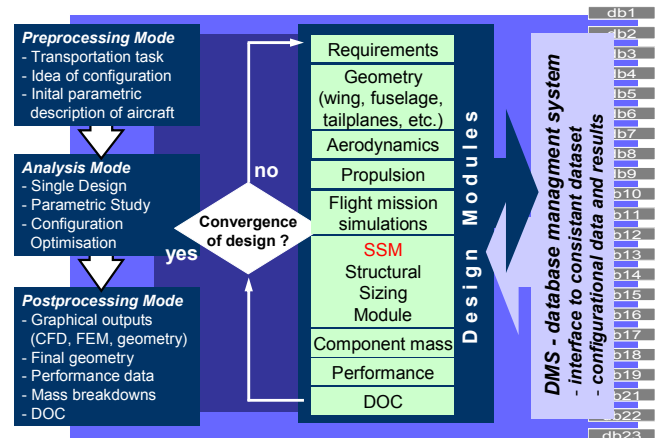


Fig. 2. Preliminary Aircraft Design and Optimization Program PrADO

4. A propulsion sizing and engine characteristics calculation is performed. A thermodynamic cycle model is used to size the engines - including a geometry and mass estimation - based on the latest thrust requirements from performance checks. Additional results are engine maps with thrust and fuel consumption data for the flight regime. The scalable performance of the engine, working like a “rubber engine”, assures adaptability to all requirements.
5. Flight mission simulations are undertaken in order to create performance data and to determine the required fuel masses for prescribed missions.
6. The Structural Sizing Module (SSM, Fig. 4) includes a Multi Model Generator (MMG) that creates a structural model (FEM) and an aerodynamic surface panel model (CFD) simultaneously. Loads are predicted and applied to the structure. A sizing process, based on stress and deformation results, is performed

iteratively with an in-house FE code or alternatively with MSC.Nastran.

7. Component masses for systems, primary and secondary structures are calculated. Structural mass is based on the sized FE model with additional corrections to account for sealants, paints and other omitted details of the FE model.
8. Direct Operational Costs are calculated for the life-cycle of the aircraft based on economical data, aircraft masses and performance data. The statement of cost include depreciation, insurance, fuel, maintenance, crew and fee.
9. Satisfaction of design boundaries (e.g. compliance with take-off and landing distances) is controlled and, if run in optimization mode, a merit function calculated. The design process restarts at step 1 unless convergence of dependent variables (e.g. static thrust, OEW) is achieved.

3.2 Aircraft Geometry Modules

As described in chapter 3.1, the PrADO geometry modules provide the geometric description of the aircraft.



Fig. 3. Examples of parametric aircraft models, PrADO

Based only on independent variables, a detailed description of the cabin (incl.

furnishings), primary structure (ribs, spars, frames, etc.), fairings and leading/ trailing edge devices is generated. This information is available via interface routines to all modules of PrADO. Fig. 3 gives examples of a conventional aircraft and one BWB variant.

In order to handle BWB configurations, the same core routines as in the conventional aircraft design, were used. Based on knowledge patterns, routines for BWB specific components, like cabin sidewise bulkheads and fuselage ribs, were added.

3.3 Structural Sizing & Mass Prediction

The Structural Sizing Module (SSM, based on work done by C. Österheld [12]) performs a physics-based mass prediction of the aircraft.

The SSM is composed of different segments as shown in Fig. 4 and additional routines that provide an interface between these segments. The relevant input data is accessed via the PrADO database management system (DMS).

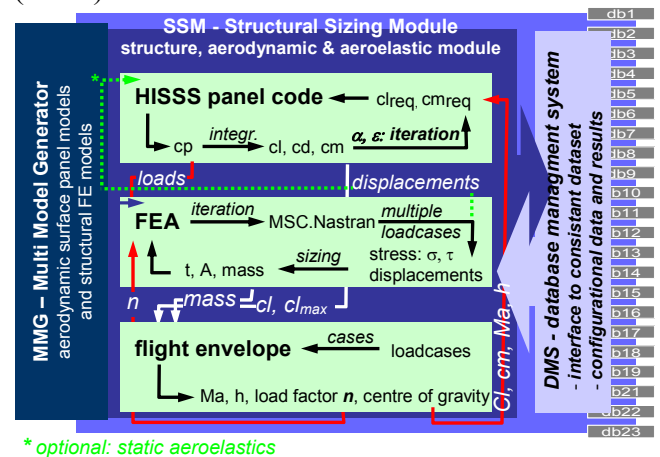


Fig. 4. Flow of information in the SSM

3.3.1 Load Prediction

In order to size the structure, a consideration of different load cases is essential. The implemented method calculates maneuver and gust accelerations (according to FAR25 specifications) for different flight situations. Each flight situation is characterized by a specific loading condition, including its corresponding aircraft mass and centre of gravity. In order to find the maximum gust or

maneuver accelerations, a calculation of the flight envelope for each loading condition would be necessary. For the purpose of saving calculation time, only certain points of the envelope are computed. These predefined points are used for the calculation of aircraft accelerations and subsequently for the definition of 9 load cases (Tab. 1).

LC	total mass	loading scenario	altitude	load factor
1	MTOW	max. payload	max	max. pos. accel. at design speed (gust or maneuver)
2	MZFW		65%	
3	MTOW	max. payload	0	
4	MLW	zero payload	0	
5	MLW	max. payload	0	
6	MZFW	MZFW-OEW	0	max. pos. accel. at cruise speed (gust or maneuver)
7	MTOW	max. payload (forw. c.g.)	max	min. neg. accel. at cruise speed (gust or maneuver)
8	MTOW	max. payload (aft c.g.)	0	
9	½ (MTOW + MZFW)	max payload	max	cruise (n=1)

MTOW (max. take-off weight)
MZFW (max. zero fuel weight)
MLW (max. landing weight)
OEW (operating empty weight)

Tab. 1. Load cases for structural sizing

The pressure distribution of each load case provides the aerodynamic loads of the FE model. In order to determine pressure distributions for trimmed flight conditions, the panel code HISSS is used to calculate the lift and pitch moment for the different angles of attack (α), trim device deflections (ε), Mach number (Ma) and flight altitude for each load case (LC).

This calculation has to be repeated several times in order to find a solution that meets the required trim and lift conditions,

$$load\ cases\ LC = 1, \dots LC_{max} :$$

$$c_{l,required}(LC) = c_{l,BWB,trimmed}(Ma, \alpha, \varepsilon) \quad (1)$$

$$c_{m,required}(LC) = c_{m,BWB,trimmed}(Ma, \alpha, \varepsilon)$$

with the following breakdown of aerodynamic coefficients:

Lift

$$c_{l,BWB,trimmed}(Ma, \alpha, \varepsilon) = c_{l,BWB}(Ma, \alpha) + c_{l,trim\ device}(Ma, \varepsilon) \quad (2)$$

Moment

$$c_{m,BWB,trimmed}(Ma, \alpha, \varepsilon) = c_{m,BWB}(Ma, \alpha) + c_{m,trim\ device}(Ma, \varepsilon) \quad (3)$$

The nonlinear relationship between angle of attack and the aerodynamic coefficients (c_l , c_m) requires at least 4 calculations to meet the trim condition.

Due to the computation time for one solution (one constant angle of attack and Mach number) of 15 min, performed on a Pentium IV 2.6 GHz, 1 GB RAM, a restart of HISSS is performed from the previous aerodynamic influence coefficient matrix (AIC). The small changes of the trim device deflection are included in the boundary conditions of panels and wakes. In this manner the calculation of the pressure distributions of 9 load cases still requires about 3 hours and has to be repeated for every global design loop until a converged design is achieved (time data based on calculations performed for one of the configurations presented in chapter 5).

3.3.2 Multi Model Generator

The aerodynamic surface panel models are created by a segment of the SSM called the Multi Model Generator (MMG). It creates models for the aerodynamic analysis and the Finite Element analysis on the basis of a consistent description of the aircraft geometry provided by the PRADO DMS.

The model generation capabilities have been created and described in [12] but changes were required to handle the new BWB configurations. The parametric mesh generation has been extended by (see Fig. 5)

- inclusion of centre body ribs (walls) dividing the cabin in compartments.
- creation of a wing transition structure.
- restriction of the cabin with additional curved bulkhead structures at the cabin sides.

- implementation of a trim device as an aerodynamic surface and as an additional structural component.
- generation of landing gear bays, their surrounding pressure bulkheads and keel beam structure.

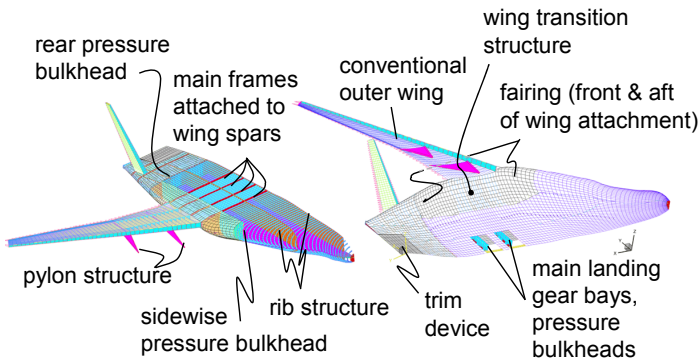


Fig. 5. Finite Element Models created with the MMG

A detailed description on the representation of structural solutions in the preliminary design models is given in chapter 4.

Depending on the chosen mesh density and aircraft size, a complete aircraft half-model in this preliminary design tool can reach around 25000 to 30000 Finite Elements.

An example of a Finite Element Model and its corresponding aerodynamic surface panel model is shown in Fig. 6.

3.3.3 Load Transfer

The transfer relationships of the aerodynamic loads from the aerodynamic surface panel model to the structural FE model are created only once for all load cases. The conditions and the method for the transfer are described in details in [12]. The basic idea is the creation of a transfer mesh that includes all structural elements that are located on the wing or body outer surface. This mesh is extended by adding (dummy) elements wherever structural elements have been omitted in the structural idealization (e.g. leading and trailing edge of wing).

The forces at the nodes of the transfer mesh are created by mapping the pressure of each panel to the corresponding GAUSS point of the interpolation mesh. The different pressure loads on each GAUSS point are used to create forces on each node of the element by

integration over the elements surface. The numerical integration of the pressure and the shape function is performed through a GAUSS quadrature. The loads of the transfer mesh and the structural mesh are chosen to be in most areas identical, which facilitates the force transfer. Loads on dummy elements of the transfer mesh are applied to the structural model by transferring the forces to the closest node of the structural model.

3.3.4 Sizing Iteration

All defined load cases (as shown in Tab. 1) are taken into account for the sizing iteration. Each element of the Finite Element model is treated as an independent design variable. Groups of elements form design regions that share a common definition of material properties, design allowables and sizing constraints. An aircraft half-model can include more than 100 of such design regions. This enables e.g. differentiation between the wing upper and lower cover properties, between floor and frame properties, or spar material behavior.

The approach to solve the sizing task is a modified fully stressed design (FSD), that complies in general with the boundary conditions (max. stress level) and side constraints (minimum and maximum sheet thicknesses or cross section area) but might not lead to a global minimum weight.

The sizing starts with initial dimensions for all elements. A strength criterion (FSD) is chosen,

$$n = 1, \dots, n_{total} \quad n \in n_g$$

$$\frac{\sigma_{vMises}(n)}{\sigma_{allowable}(n_g)} \leq 1 \quad (4)$$

with

$$\sigma_{vMises} = \sqrt{\sigma_x^2 + \sigma_y^2 - \sigma_x \sigma_y + 3\tau_{xy}^2}$$

$$n \dots element \quad (5)$$

$$g \dots design region$$

that is fulfilled by almost all elements of the model. A small number of elements is allowed to violate the stress constraints with the purpose of saving computing time. To improve the

stability of this sizing procedure, damping has been introduced into the sizing method.

The fully stressed design is applicable to metal designs and has led, in combination with additional factoring (chapter 3.3.5), to good correlations with actual aircraft weights (see examples for AIRBUS aircraft in [12]). The anisotropic parts of the structure (skin and smeared stringers) are sized by their isotropic part. The ratio of skin- to stringer-area remains constant. Future investigations are planned to include composites, but rather than substituting material properties (like in [1]), different sizing approaches are needed as well. This difficulty and the lack of comparability to today's aircraft has limited our approach to the current state.

3.3.5. Weight Prediction

The mass of the primary structure is determined from the volume of the Finite Elements. A weight correction is performed by adding specific masses (mass/area or mass/length) to represent paint, sealants, manholes, etc.

4 Structural Solutions for BWB Aircraft

The model generation capabilities of the MMG were limited to conventional aircraft designs. The parametric description of the aircraft requires typical arrangement patterns that are implemented as knowledge patterns in

subroutines.

BWB specific subroutines have been implemented for the creation of structural details in order to correctly include all major contributors to the primary structural mass. An additional challenge in the implementation of such methods is to know how certain details should be designs. The concepts and solutions presented in the following paragraphs are shown for illustration purposes; their structural efficiency might be improved by detailed studies, but nevertheless, their estimated weights are supposed to be rather conservative.

4.1 Cabin Structure

The cabin of BWB aircraft has in general a large width in span wise direction. Considerations of comfort and evacuation are likely to be a limiting factor for the width of the cabin. Due to the necessary pressurization of the cabin, the loading of the structure leads to high bending loads in the upper and lower, almost flat, parts of the cabin. This effect can be reduced by structural elements carrying the vertical force components as shown in Fig. 7.

The need for structural components connecting the upper and lower side of the fuselage is thus obvious. Other details about efficient structural designs for BWB shell configurations are less evident (necessity of

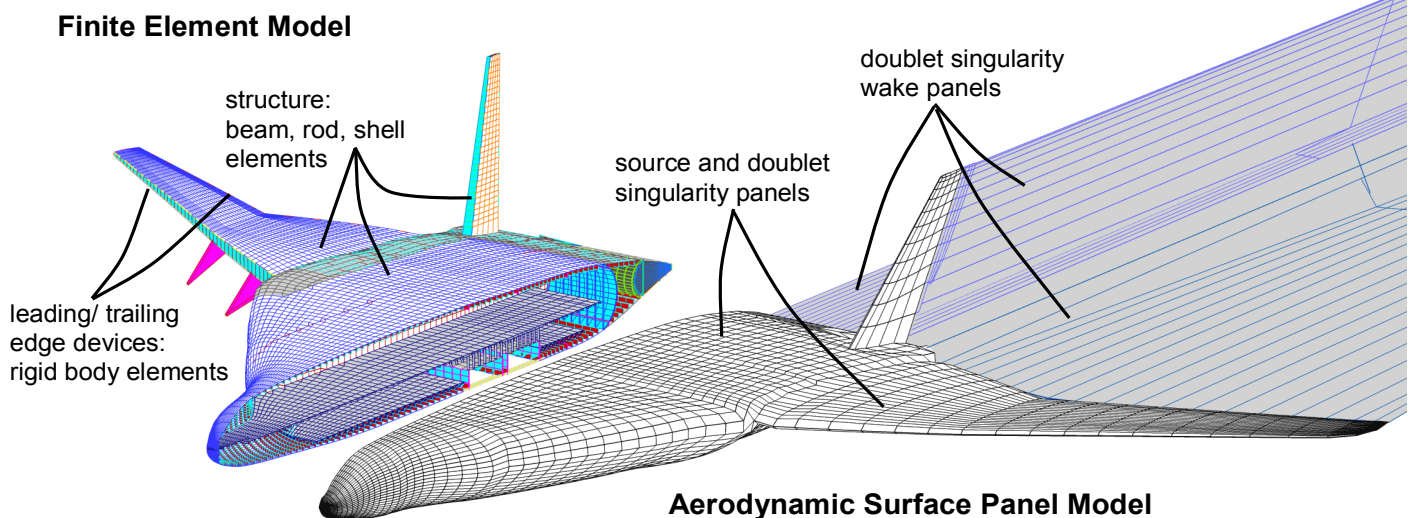


Fig. 6. Parametric models (aerodynamic and structure)

tension struts, stiffeners, single, double or sandwich layouts).

Very few concepts of BWB shell design for upper and lower cabin shells have been published in detail. Many of the presented solutions (e.g. [1], [13]) refer to the same structural concept presented by Liebeck in [6] where a “BWB separate pressure shell” and a BWB “integrated skin & shell” is described. A similar proposal is found in [2].

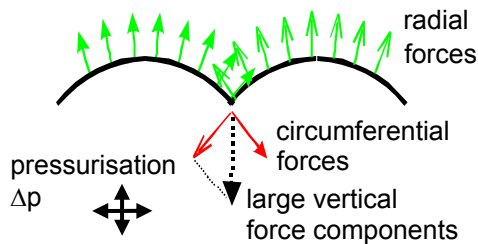


Fig. 7. Resulting loads at shell interaction

Other solutions are presented by Mukhopadhyay in [9] and [10]: A multi-bubble layout, with an additional inner curved skin and a ribbed structure or honeycomb core between inside and outside skin, is presented.

Nevertheless, it does not become clear, which criteria drives the designs: A double skin layout seems to be favorable, if pressurization loads are carried by an inner membrane. However, in the case of disturbed deformation (e.g. limitation in deformation due to little available space), the membrane loads become less important and the bending moments in the structure dominate. Consequently, a pure membrane shell design requires a construction that decouples the inner membrane and the outer skin.

In detail, this decoupling of inner and outer structure might be impossible and hence a double skin structure, with a connection between the skins (honeycomb core, frames), evolves from the basic inner membrane idea. This structure will certainly show a different characteristic in carrying the loads (high bending stiffness – little deformations).

Investigations in [4] have shown no clear advantage for the double skin in comparison with single skin layouts. The results presented in [4] have been limited to metal design with a

classical, rectangular arrangement of stringers and frames. The pressure loads are rather carried by a bending resistant structure than by a flexible membrane. The inner skin is thus superfluous and its function is reduced to increase the section modulus.

An improvement of rigidity can be achieved by using thick sandwich structures, as shown [9] and [10].

In order to create comparable results it has been decided to remain with a single skin metal layout for the presented investigations. This enables a fair comparison between BWB results and conventional aircraft in application with a well established criteria for sizing and weight prediction. Inclusion of sandwich structures is planned for future activities.

Currently the lower and upper skin is modeled with shell elements and additional frames with beam elements. The membrane stiffness of the shell elements is chosen to be anisotropic to include the stiffness of arbitrary stringer orientations. In order to enhance the model, a further implementation of shear and bending stiffness is possible. Consequently, different single, double or sandwich panels may be represented by a combination of weight specific membrane, shear and bending properties.

An implementation of additional walls in the model was unavoidable. These walls connect the upper and lower skin and are constructed of membrane and beam elements (see Fig. 8).

The front, rear and side of the cabin is closed by pressure bulkheads (Fig. 8). These structures are modeled by membrane elements and additional tension struts in the chord.

Non-structural masses are included in the FE model as mass points that are attached to the floor with multi point constraints. The mass distribution and amount is provided for different load cases by the PrADO database.

4.2 Landing Gear Bay

The undercarriage is not part of the structural model. Its loading is introduced (in a landing

REPRESENTATION OF STRUCTURAL SOLUTIONS IN BLENDED WING BODY PRELIMINARY DESIGN

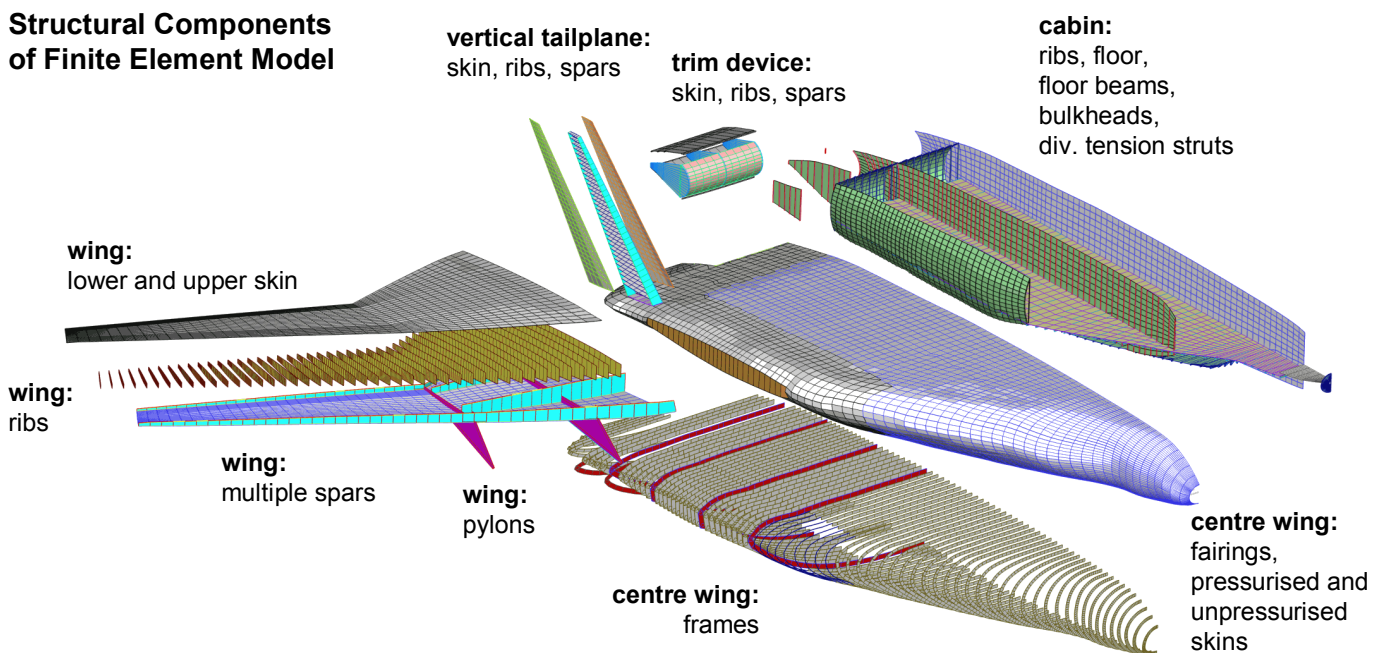


Fig. 8. Exploded view of structural components of the Finite Element Model

impact load case) into the structure via rigid body elements.

The landing gear bay structure might have more influence on the structural mass due to the cabin pressurization. A configuration with landing gear cut-outs in the fuselage is shown in Fig. 6 and 9. The sides of the bay are closed by flat bulkheads and the top of the bay by a jagged bulkhead structure. (supported by the floor via struts). A keel beam structure has been introduced to compensate for the interrupted longitudinal load path.

4.3 Rear Fuselage Trim Device

The sizing of the structure is performed with aerodynamic loads computed by an aerodynamic panel code. In order to create balanced loading of the FE model, aerodynamic trim loads are necessary. This demand is fulfilled by a trim device, which was first introduced in the aerodynamic panel model only. In addition to these changes, a simple rudder concept has been included in the mesh generator for the structural model (Fig. 9 and 11) as well. The trim rudder is composed of a simple rib and spar structure and connected by an axle to the fuselage structure. All parts of the rudder, including the axle, are part of the sizing process.

4.4 Wing Transition Structure

The wing attachment to the fuselage has been changed from the typical centre-box wing-attachment to an alternative type. The loads are introduced into the fuselage through a transition structure comprised of shear walls connected to the fuselage frames.

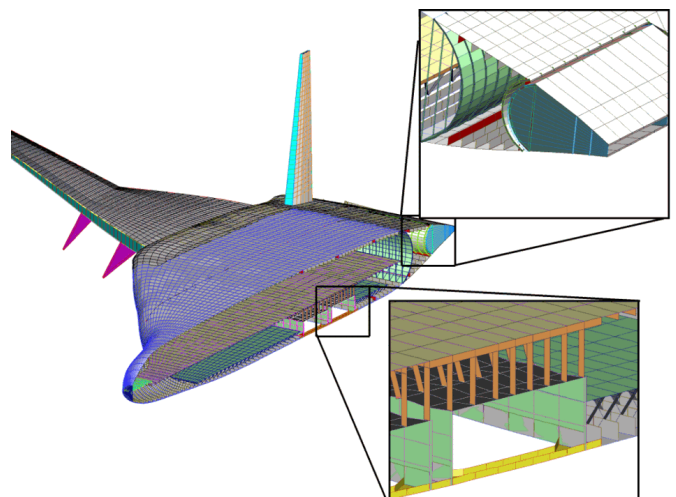


Fig. 9. Rear trim device and landing gear bay structure

5 Application and Results

The Blended Wing Body configuration used for this investigation has been chosen arbitrarily

for illustration purposes of the structural and aerodynamic modeling capabilities.

This configuration has been computed with the integrated design tool PrADO until convergence of dependent aircraft variables (e.g. max. take-off weight, fuel weight) have been achieved.

Some of the assumed design requirements are given in Tab. 2.

span	≤ 100 m
(fuselage) length	≤ 52 m
design range	14200 km
design payload	700 PAX (3-class layout) ~ 66500 kg
max. payload	~ 100110 kg
cruise Mach number	0.85
engines	comparable to <i>Engine Alliance GP7200</i>
max. take-off length	≤ 3300 m

Tab. 2. Design requirements (extract)

Based on these inputs three convergent aircraft have been calculated, that differ in the number of ribs in the fuselage. Results are presented in Tab. 3 and 4.

The displacements and the stress distribution are different for each load case. Fig. 10 shows results of load case 1 (load case numbering referring to the Tab. 1 definition) after sizing has been performed.

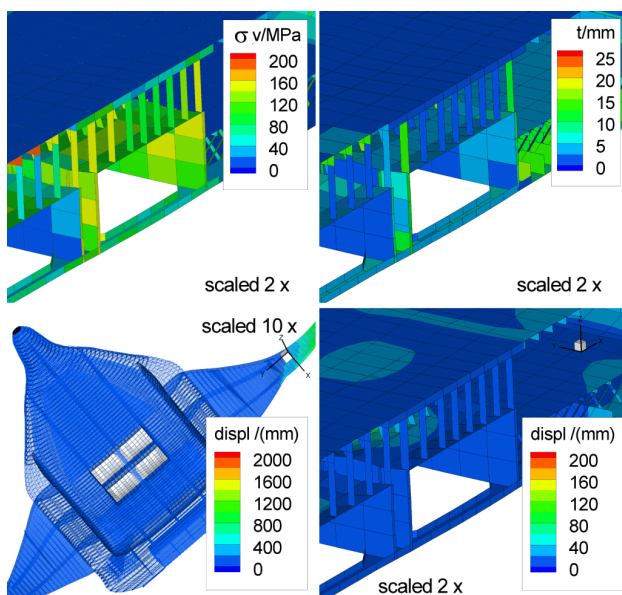


Fig. 10. Von Mises stress, displacements of load case 1 (max. positive load factor, max. differential pressure) and element thicknesses after sizing, 4 bays

The upper half of the figure is a fringe plot of the von Mises stress (σ_v) distribution and the skin thicknesses (t) after sizing. Due to the way skin and stringer are modeled, the thicknesses shown in the figure always belong to a combined skin and stringer shell thickness. The lower half shows the displacements in parts of the landing gear bay and the complete aircraft. As expected, the pressurization of the landing gear bay introduces large tension loads in the supporting struts and into the neighboring floor structure. The maximum stress level varies, depending on the components' allowable stress. The pressurized skin has been chosen to remain under a fatigue critical stress level of 100 MPa.

Figure 11 shows details of the deformations, thickness distributions and the von Mises stresses in the rear end of the fuselage. The stress distribution in the skin and the bulkhead is shown in the upper left image. Again the stress in the skin remains below 100 MPa. Due to aerodynamic loads, the trailing edge of the rear trim device deforms up to 200 mm in load case 1 and might require additional stiffening of the rudder and its connection to the fuselage.

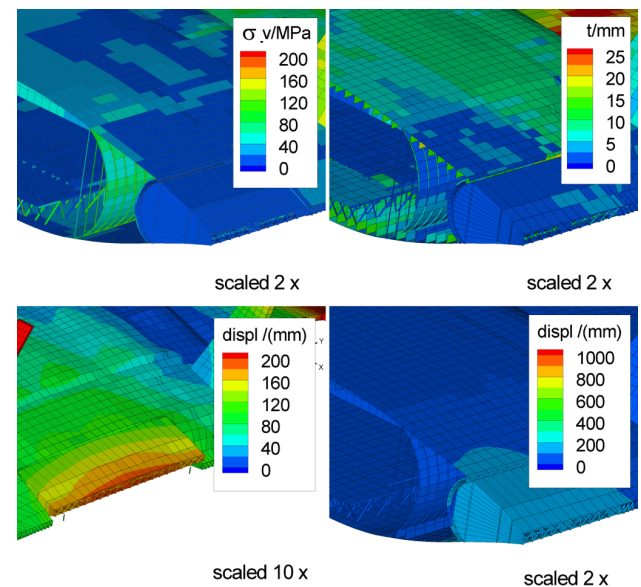


Fig. 11. Von Mises stress, displacements of load case 1 (max. positive load factor, max. differential pressure) and element thicknesses after sizing, 4 bays

A stress, deformation and skin thickness plot of the complete aircraft is depicted in Figure 12. The stress plot shows, that the stress

level in the wing is allowed to be higher than in the (pressurized) parts of the fuselage. The deformations of the pressurized cabin (shown in the lower half of the figure) are scaled by a factor of 20 to show the bending in the skin between the ribs of the centre body. To give an overview on how the deformation changes with the number of ribs, additional plots are given in the appendix (Fig. 14: 4 bays, 5 bays and 6 bays displacement plots).

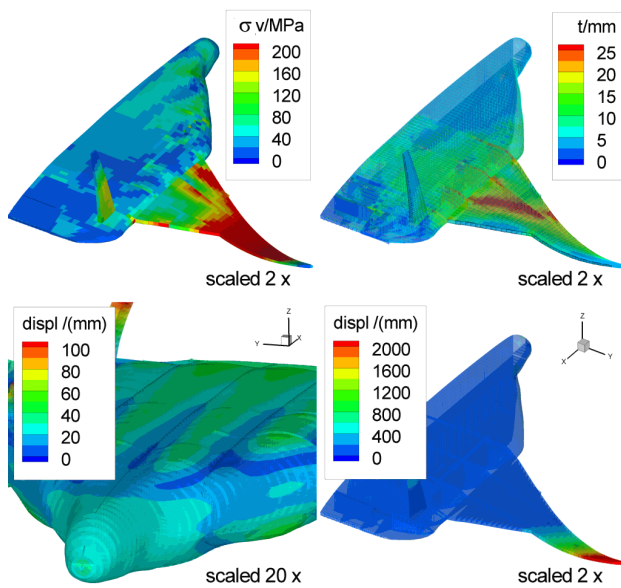


Fig. 12. Von Mises stress, displacements of load case 1 (max. positive load factor, max. differential pressure) and element thicknesses after sizing, 4 bays

The result of the aircraft design process with the tool PrADO shows differences between the three investigated configurations. With the same design requirements, the differences in the structure lead to different loading conditions and consequently to different structural masses. Due to the closed design loop, these results create consequences in almost every discipline.

Tab. 3 shows an extract of the detailed mass breakdown. The configuration with 6 bays has the lowest structural weight, although more walls are required than for the 5 bay, or 4 bay variants. The smaller skin panels between two walls lead to lower bending moments and hence to lower structural weight of the skin. In addition, lower weights in parts of the structure, that are not directly related to the number of ribs, can be observed. This is due to the lower

overall weight of the aircraft (landing impact load case) and due to the positive stiffening effect of the walls on the global deformation of the centre wing.

In total, a difference of almost 10000 kg in fuselage weight lies between the 4 bay and the 6 bay solution (after a complete, iterative design process with PrADO). A further increase in the number of bays does not seem to be feasible due to their negative effect on cabin layout and space requirements.

	4 bay cabin	5 bay cabin	6 bay cabin
vertical tail plane /(kg)	4465	4466	4476
fuselage structure /(kg)	108458	104751	98877
- fuselage ribs	5652	6516	6575
- landing gear bays	3344	2915	2865
- cabin-side bulkheads	4172	4279	4297
- fuselage trim device	2149	2064	2064
- other components (e.g. frames, skin, floor, wing attachment, etc.)	93141	88977	83076
wing structure /(kg)	53664	53388	52700
pylons /(kg)	6554	6383	6207
landing gear /(kg)	20403	19867	19180
total structure mass /(kg)	193544	188855	181440

Tab. 3. Structure mass chapter of convergent designs

The global masses of the convergent designs are given in Tab. 4.

	4 bay cabin	5 bay cabin	6 bay cabin
manufacturer empty weight /(kg)	264492	257928	248635
operating empty weight /(kg)	292709	286145	276852
max takeoff weight /(kg)	702144	688452	673338
fuel @ design range (incl. reserve) /(kg)	342935	335807	329986

Tab. 4. Aircraft masses of convergent designs

The results after convergence of the design process point out, that additional adjustment work is necessary to improve the configuration. Especially the position of the centre of gravity (c.g.) and the corresponding, necessary trim device deflections, increase the induced drag and thus decrease the lift/drag ratio in cruise condition. As a consequence, the fuel mass and the overall aircraft mass

increases and further penalizes the configuration.

In the appendix, plots of the pressure distribution (Fig. 13) and of the lift/drag ratio (Fig. 15) of the trimmed configuration for different positions of the c.g. are shown. A maximum lift/drag ratio of 21 is shown (for c.g. positions between 34 m and 36 m). Further configuration modifications are likely to improve this value and the overall performance.

6 Conclusion

The evaluation capabilities in the case of Blended Wing Body aircraft of the preliminary design program PrADO have been enhanced by structural details in the weight prediction models. A physics-based mass prediction, including a consideration of the real geometry, is incorporated and provides possibilities for fast multidisciplinary analyses.

The boundary conditions of the Finite Element model are defined by a large number of load cases, each including a detailed aerodynamic pressure and a specific mass distribution. Referencing the successful approach for conventional aircraft mass estimation (shown in [12]), a method for preliminary BWB studies is created.

Future changes to the method are necessary including an implementation of additional sizing constraints, of composite structures and appropriate sizing methods. In addition, improvements of the robustness of the mesh generation process are necessary.

References

- [1] Bradley K. A Sizing Methodology for the Conceptual Design of Blended-Wing-Body Transports, NASA/CR-2004-213016, Sept.2004.
- [2] Demitriev G, Shkadov L et al. The Flying-Wing Concept – Chances and Risks, *AIAA/ ICAS International Air and Space Symposium and Exposition: The next 100 years*, Dayton, AIAA 2003-2887, 2003.
- [3] Fornasier L. A Higher-Order Subsonic/Supersonic Singularity Method for Calculating Linearized Potential Flow, *23rd Aerospace Sciences Meeting & Exhibit*, Reno, AIAA 84-1646, 1984.
- [4] Hansen L, Horst P. Strukturkonzepte in konventioneller und zweischaliger Bauweise für flache nichtzylindrische Rumpfkfigurationen, *DGLR Jahrestagung*, Dresden, Jahrbuch Band III, 2004.
- [5] Heinze W. *Ein Beitrag zur quantitativen Analyse der technischen und wirtschaftlichen Auslegungsgrenzen verschiedener Flugzeugkonzepte für den Transport großer Nutzlasten*, PhD-Thesis TU Braunschweig, ZLR Forschungsbericht 94-01, 1994.
- [6] Liebeck R.H. Page A.M, Rawdon B.K. Blended-Wing-Body Subsonic Commercial Transport, *36th Aerospace Sciences Meeting & Exhibit*, Reno, AIAA 98-0438, 1998.
- [7] Liebeck R.H. Design of the Blended-Wing-Body Subsonic Transport, *40th AIAA Aerospace Sciences Meeting & Exhibit*, Reno, AIAA-2002-0002, 2002.
- [8] Liebeck R.H. Design of the Blended Wing Body Subsonic Transport, *Journal of Aircraft*. Vol. 41, No. 1, pp. 10-25, 2004.
- [9] Mukhopadhyay V. Sobieszcanski-Sobieski J., Analysis Design and Optimization of Non-cylindrical Fuselage for Blended-Wing-Body (BWB) Vehicle, *9th AIAA/ ISSMO Symposium on Multidisciplinary Analysis and Optimization*, Atlanta, AIAA 2002-5664, 2002.
- [10] Mukhopadhyay V. Blended-Wing-Body (BWB) Fuselage Structural Design for Weight Reduction, *46th AIAA/ ASME/ ASCE/ AHS/ ASC Structures, Structural Dynamics and Materials Conference*, Austin, AIAA 2005-2349, 2005.
- [11] Österheld C, Heinze W, Horst P. Preliminary Design of a Blended Wing Body Configuration using the Design Tool PrADO. *Proceedings of the CEAS Conference on Multidisciplinary Aircraft Design and Optimisation*, Cologne, 25./26. June 2001.
- [12] Österheld C. *Physikalisch begründete Analyseverfahren im integrierten multidisziplinären Flugzeugvorentwurf*, PhD-Thesis TU Braunschweig, ZLR Forschungsbericht 2003-06, 2003.
- [13] Wakayama S, Kroo I. The Challenge and Promise of Blended-Wing-Body Optimization, *7th AIAA/ USAF/ NASA Symposium of Multidisciplinary Analysis and Optimization*, St. Louis , AIAA-98-4736, 1998.

7 Acknowledgments

Part of the work presented was funded by the 5th framework program of the European Union during the project VELA (very efficient large aircraft).

Thanks is extended to L. Fornasier/EADS-M for providing the HISSS panel code.

8 Appendix

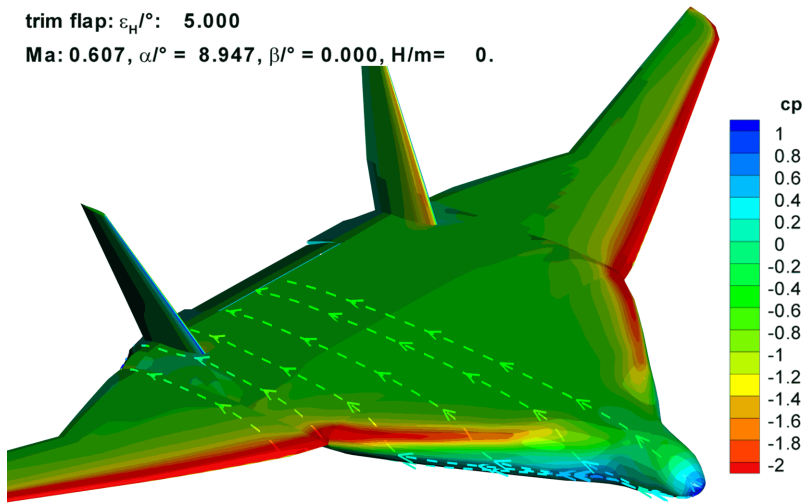


Fig. 13. Pressure distribution at Ma 0.607, angle of attack = 8.947°, trim flap deflection = 5°

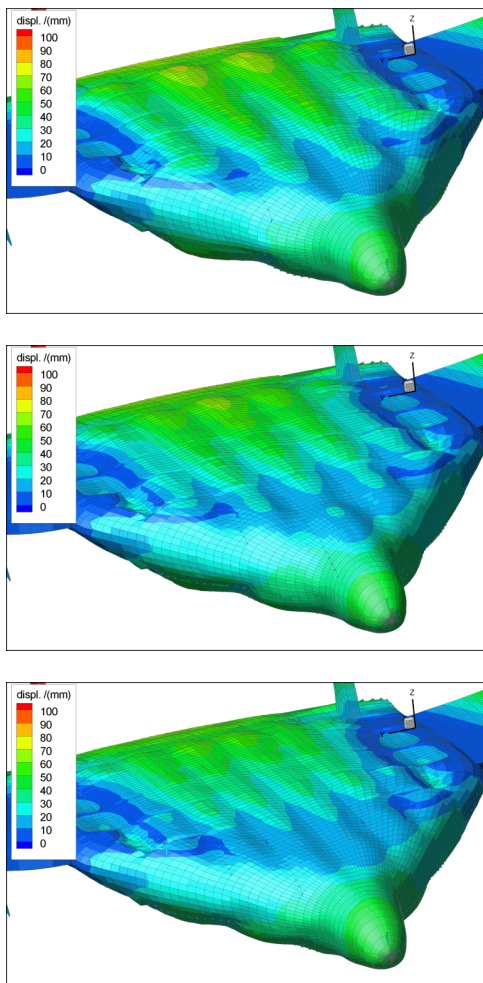


Fig. 14. Scaled deformation (20x) at cruise condition:
4 bays (top), 5 bays and 6 bays (bottom)

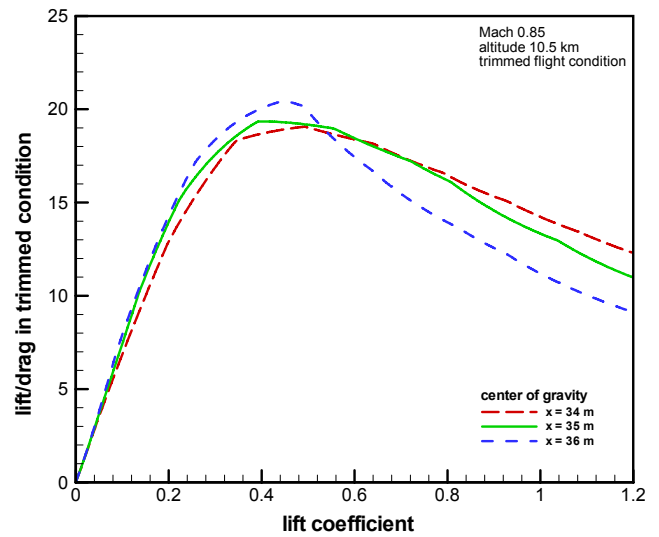


Fig. 15. Lift/drag ratio at cruise (Ma 0.85, alt. 10.5 km)
as a function of the lift coefficient and c.g. position